(英1)

Non-linear Finite Element Analysis of Deep Beams

Analyse non-linéaire par éléments finis de poutres de petite portée

Nichtlineare Finite-Elemente-Berechnung von hohen Trägern

JUNICHIRO NIWA
Graduate Student
University of Tokyo
Tokyo, Japan

KOHICHI MAEKAWA
Graduate Student
University of Tokyo
Tokyo, Japan

HAJIME OKAMURA
Associate Professor
University of Tokyo
Tokyo, Japan

SUMMARY
A non-linear finite element method of analysis was applied to predict the behavior of reinforced concrete deep beams. The behavior of concrete including strain softening tendency and anisotropy was modelled by the total strain theory and combined with non-linear analysis. The analytical results were compared with the experimental results. The techniques for the non-linear method of analysis and the capability to predict the behavior of deep beams were investigated.

RÉSUMÉ
Le comportement non-linéaire de poutres en béton armé de petite portée est analysé par éléments finis. Le comportement du béton, comprenant l'anisotropie et le "strain-softening", est simulé par la théorie de la déformation totale combinée à l'analyse non-linéaire. Les résultats analytiques furent comparés aux résultats expérimentaux. Les techniques d'analyse non-linéaire et la capacité de prédiction du comportement de poutres à petite portée sont analysées.

ZUSAMMENFASSUNG
Eine nichtlineare Finite-Elemente-Methode wurde auf die Berechnung von hohen Tägern aus Stahlbeton angewandt. Das Verhalten mit Einschluss von Steifigkeitsabnahme und Anisotropie wurde mit einer nichtlinearen Berechnung kombiniert. Theorie und Experiment an hohen Trägern wurden verglichen.

1. INTRODUCTION

The behavior of reinforced concrete structures under applied loads is complex due to numerous internal load paths. Such load paths vary a great deal due to the distribution of stiffness in the structure, and that variation in stiffness arises from variable pattern and sequence of crack occurrence and plastification of materials. On the other hand the whole picture of the constitutive law of concrete is not yet apparent particularly when the combination of applied stresses changes as they are increased. The various factors influencing the behavior of reinforced concrete structures are interlaced and therefore, any devised methods of analysis need be scrutinized in the lights of experimental observations [1].

A finite element method of analysis with a few techniques to overcome the difficulties characteristic to nonlinearlity was presented to predict the behavior of reinforced concrete deep beams and the analytical results were compared with the experimental results specially tested for this purpose.

2. NUMERICAL METHOD

In the analysis step iterative procedure for non-linear finite element method was used. In applying the analysis to deep beams, enforced displacements were imposed because of the easier evaluation of the ultimate strength. The general flow of the main routine is as shown in Fig.1.

At the first iteration of each step, the equivalent nodal forces, which appear when constraint displacements are applied to the structures, are calculated using the updated stiffness matrix in the preceding step. During iterative routine, the stiffness matrix was formed at each iteration. The increments of nodal displacements are then calculated.

$$u = K^{-1}\Delta F \tag{1}$$

$$\Delta F = F - \iiint B^T \sigma \, dv \tag{2}$$

K : global stiffness matrix , F : equivalent nodal force
F : total external nodal forces, F=0 in this analysis
B : strain displacement matrix , σ : stresses

In each iteration, the unbalanced forces are calculated by equation 2. If unbalanced forces are not as small as required, the next incremental displacements are calculated by setting the equivalent nodal forces as the unbalanced forces. When the value of unbalanced force differs from that of previous iterative routine significantly or the direction of the force changes, the nodal force increment for correction is made one half the corresponding unbalanced force. The selection of one half is arbitrary, but by this procedure, the risk of divergence or a great leap beyond equlibrium points was avoided to some extent.

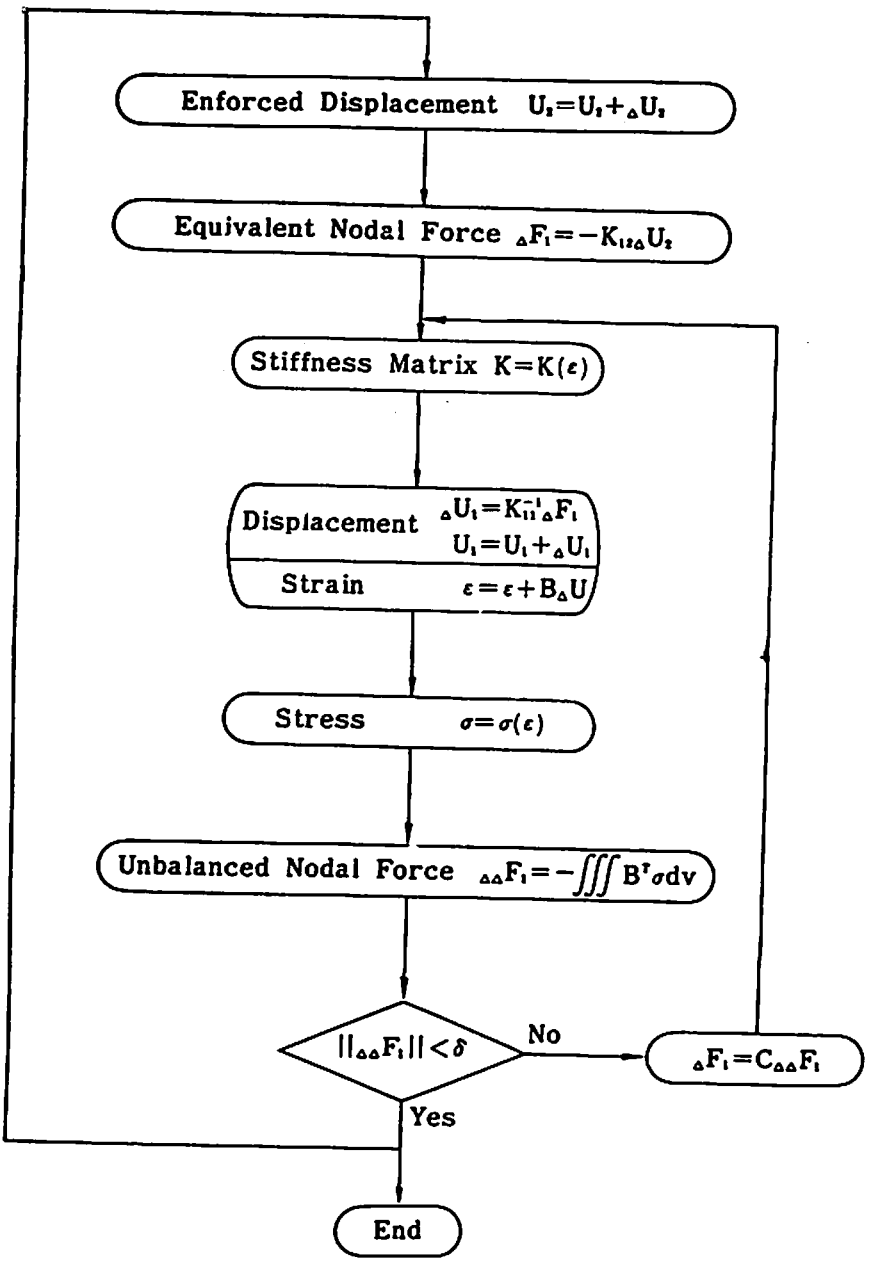

Fig. 1 General Flowchart of Non-linear Iterative Routine

3. CONSTITUTIVE EQUATIONS OF CONCRETE

3.1 Stress strain relationship of concrete

There exist two families of constitutive formulations according to the method of stress evaluation, namely differential and total strain formulation. The former evaluates stresses by integrating stress increment at each step. The total strain formulation calculates stresses by total strains and constitutive equations which contain invariants with regard to coordinate transformations as parameters. In the analysis the total strain formulation was used for evaluating stresses for the following reasons.
(a) Strain softening tendency under multiaxial stress states is easily modeled.
(b) No accumulation of errors in estimating the stresses occurs so that the step size can be set relatively large.
(c) Experimental data are directly used for making the constitutive equations.

The constitutive law used for the analysis of deep beams is two dimentional, and the following scalar values named equivalent stress and equivalent strain which are indicated by stress and strain invariants with regard to coordinate transformations are defined.

$$s = s(\sigma_{ij}) = s(\sigma_1, \sigma_2) = \sqrt{\left(\frac{\sigma_1+\sigma_2}{2.32fc}\right)^2+\left(\frac{\sigma_1-\sigma_2}{1.108fc}\right)^2} \quad (3)$$

$$e = e(\varepsilon_{ij}) = e(\varepsilon_1, \varepsilon_2) = \sqrt{\left(\frac{\varepsilon_1+\varepsilon_2}{9.6\times10^{-4}}\right)^2+\left(\frac{\varepsilon_1-\varepsilon_2}{6.2\times10^{-4}}\right)^2}\Big/\sqrt{fc} \quad (4)$$

where s : equivalent stress, e : equivalent strain
fc : uniaxial compressive strength, assumed as 90% of the cylinder strength [2]
σ_1 σ_2: principal stresses ($\sigma_1 > \sigma_2$), ε_1 ε_2: principal strains

These two invariants represent the degree of stress and strain level respectively, and are introduced in order to allow the actual biaxial stress-strain curves to be expressed in an one-to-one relationship as in the case of uniaxial conditions, so that a family of uniaxial concepts of stress-strain relationships is to be used. This equation was determined by a least squares fit of biquadratic polynomial from the reported experimental data [2,3,4,5].

$$s = f(e) \quad (5)$$

$$= 1.042\ e - 2.083\ e + 0.42\ e + 2.0\ e \quad : e < e2$$

$$= -0.25\ e + 1.25 \quad : e > e2$$

The relationship of each stress and strain components in the local coordinate system whose axes coincide with the principal stress axes is developed, in consideration of anisotropic characreristics of concrete due to microcracking and void formation. These characteristics of concrete are dependent on the strain level, and

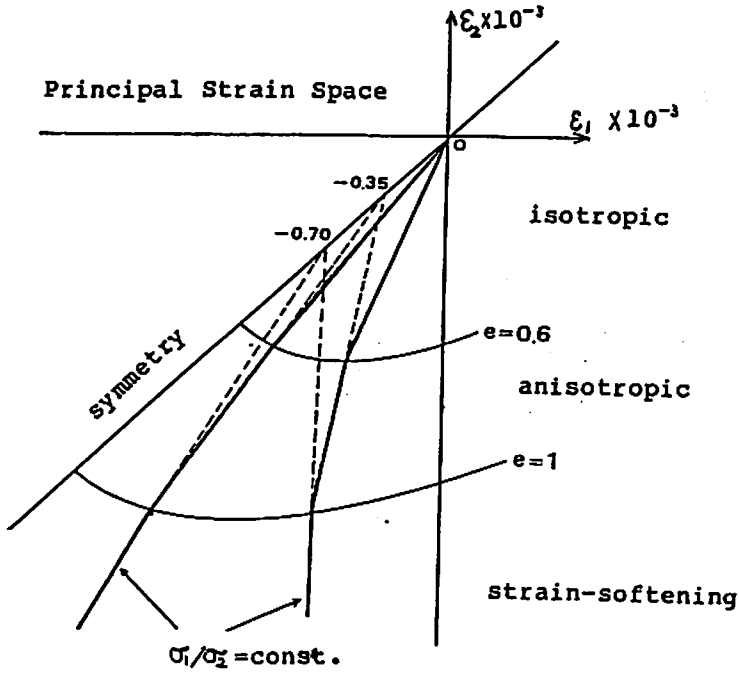

Fig. 2 Proportional Loading Pathes on Principal Strain Surface

the relationship of two principal strains under constant principal stress ratio is modeled as tri-linear one as shown in Fig.2. The relation is developed based on the reported experimental data [2], [3],[4].

In the low level of strain, concrete can be assumed an isotropic material [5] and the relation of two principal values, stresses and strains, is reasonablely assumed as the one for elastic materials.

$$p = (q + \nu)/(1 + \nu * q) \qquad (6)$$

where p : stress ratio = σ_1/σ_2 ,q : strain ratio = $\varepsilon_1/\varepsilon_2$
ν : Poisson's ratio

On increasing the strain to a high level, a stage is reached where the microcracking between aggregates and mortar starts to propagate and the anisotropic behavior appears gradually. This boundary between the isotropic and the anisotropic is assumed to depend on the value of the equivalent strain, and is assumed as 0.6 in the calculation (see Fig.2). After this stage the slope of the line which shows the relationship of the two principal strains is changed to express the anisotropic behavior of concrete. When the strain-softening level is attained (e=1), the effect of

anisotropic behavior and drastic void formation becomes significant, and the slope is changed again.

When two principal strains are given, the corresponding strain ratio at the isotropic stage is obtained by using the tri-linear relation as shown in Fig.2. Then, the stress ratio is calculated by equation 6. Using this stress ratio and the equivalent stress, which can be calculated by equation 5, each principal stress is calculated by using equation 3.

s.2 Cracking

In non-linear finite element method of analysis, there are two methods for representing the behavior of cracked concrete; discrete crack and smeared crack model. The former simulates a crack by releasing the connection of each element. The latter represents a crack by modifying the constitutive equations. The smeared crack model can simulate the total responses of structural systems in which crackings occur, and was used for the analysis of deep beams.

Criterion of cracking is determined by stresses, and cracking is defined to occur when the principal stresses make the following crack index equal to unity.

$$\begin{aligned} Ci &= (\sigma_1/ft) - \sqrt[3]{(1 + \sigma_2/fc)} \quad : \text{under compression-tension} \\ &= (\sigma_1/ft) - 1 \quad : \text{under biaxial tention} \end{aligned} \qquad (7)$$

where ft : uniaxial tensile strength

The orientation of crack is considered to be normal to the major principal stress, and the stress component normal to a crack is reduced to zero. The condition, where the crack index is zero, represents the failure envelope at compression-tension and tension-tension stress states. When the value of crack index is between zero and one, stress normal to the direction of a crack is maintained constant although the stress calculated by the above mentioned method exceeds the value corresponding to zero of crack index.

Shear transfer across the crack is simply simulated by changing the shear stiffness along the crack as shown in equation 10. Calculations were made by zero stiffness in general and half of the uncracked stiffness in some case. When the strain normal to the crack is compressive, the crack is closed and the condition is assumed to be the same as that of uncracked concrete. If concrete at an evaluation point has previous experiences of cracking, the stress component normal to the crack is calculated and the crack is assumed to open again when the stress is tensile.

3.2 Stiffness of iterative calculation

In the non-linear iterative procedures a stiffness for each evaluation point is necessary. The stiffness matrix is formed by superposing the isotropic stiffnesses of uncracked concrete and

the anisotropic stiffnesses of cracked one. The assumption of quivalent stress-strain relationship permits the evaluation of incremental elastic moduli as in equation 8.

$$E = E0 \frac{ds/de}{ds/de\,|e=0} \tag{8}$$

where E0 is the initial tangent stiffness moduli

With the tangent moduli and effective Poisson's ratio, the isotropic tangent stiffness matrix of uncracked concrete is obtained by equation 9. The anisotropic tangent stiffness of cracked concrete is written in equation 10, using the tangent moduli parallel to crack direction. The effective Poisson's ratio is also assumed as in equation 12 in consideration of the equivalent strain level.

$$\frac{E}{1-\nu^2}\begin{bmatrix} 1 & \nu & 0 \\ \nu & 1 & 0 \\ 0 & 0 & \frac{1-\nu}{2} \end{bmatrix} \tag{9}$$

$$\begin{bmatrix} 0 & 0 & 0 \\ 0 & E & 0 \\ 0 & 0 & \alpha G \end{bmatrix} \tag{10}$$

where $\alpha = 0$ or 0.5, $G = E/(2(1+\nu))$ (11)

$$\nu = \begin{cases} 0.2 & e < e1 \\ 1.75\,e - 0.85 & e1 < e < e2 \\ 0.9 & e > e2 \end{cases} \tag{12}$$

A lower limit is set for the possitive tangent stiffness, because the global tangent stiffness matrix becomes numerically unstable when diagonal terms approach zero. One hundredth of the initial tangent stiffness was used for the lower limit, after some trial calculations were executed.

4. APPLICATION TO THE ANALYSIS OF DEEP BEAMS

Reinforced concrete deep beam is one of the problems which need the help of a suitable non-linear finite element method of analysis for understanding the behavior. The applicability of the analytical method to deep beams is investigated. Deep beams used in the comparison with the analytical results were particularly tested for this purpose. The characteristics of eight specimens are shown in Table 1. The parameters such as concrete strength (13 MPa - 67 MPa), reinforcement ratio (3 % - 6 %), shear span (150 mm - 200 mm) and height of beam (300 mm - 600 mm) are widely and systematically varied. To ensure the anchorage, main reinforcing bars were bent up as shown in Fig.4. No shear reinforcement is used.

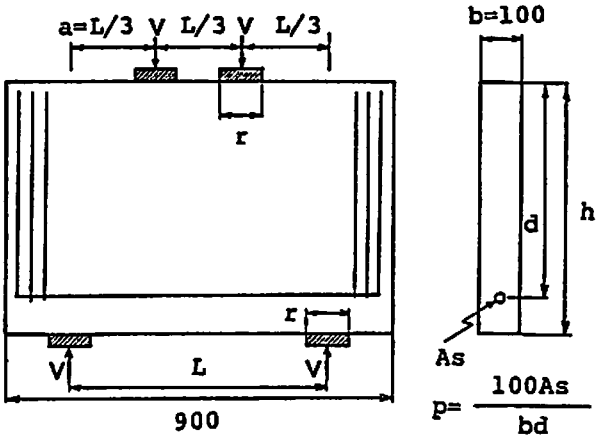

Fig. 4 Deep Beam Specimens Tested

Table 1 Characteristics of Deep Beam Specimens

Beam	a(mm)	d(mm)	a/d	r(mm)	h(mm)	p(%)	fy(MPa)	fc'(MPa)
T1	200	228	0.88	140	300	6.0	364	35.8
T2	200	507	0.39	100	600	3.0	389	54.7
T3	200	228	0.88	100	300	3.0	364	13.1
T4	150	507	0.30	140	600	3.0	389	13.1
T5	200	507	0.39	140	600	6.0	389	66.6
T6	150	507	0.30	100	600	6.0	389	35.8
T7	150	228	0.66	100	300	6.0	364	59.9
T8	150	228	0.66	140	300	3.0	364	58.8

Considering the flow of stresses in the beam, a finite number of skew quadrilateral elements as shown in Fig.5 were used for the analysis of plane stress conditions. The same topological shapes and number of elements were used for all the eight beams.

The assumption of the plane stress is considered to be reasonable for most portions of the beam. But, concrete near the bearing plate is obviously stressed triaxially and the effect on the behavior of the beam is not negligibly small, especially in the concrete mainly stressed in compression by bending moment. Therefore, five elements hatched in Fig.5 were to have an apparent higher compressive strength 1.8 times that for other elements. However, the concrete strength for the element at the span center was made normal, so that the increase of concrete strength

in triaxial compression zone might not affect the flexure dominant strength of the beam.

Eight nodes isoparametric elements were used taking into account that the strain distribution in the beam is more or less linear. Two by two stress evaluation points, or Gauss points, were arranged in each element. This number of Gauss points may ordinarily be sufficient. However, five by five Gauss points were arranged in four elements where strains have the possibility of changing from a very small magnitude to softening level within the element. The elements are marked with character 5 in Fig.5. For this kind of element, two by two points were insufficient for the evaluation of stresses.

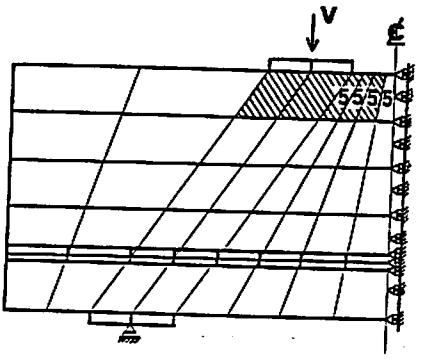

Fig. 5 Idealization of Finite Elements

Totally, 40 concrete and 12 steel elements with 174 nodes and 292 Gauss points were used. The CPU time to calculate ten steps with two iterations in each step was about 70 seconds using a HITAC M-200H system at the computer center of University of Tokyo, and the computation fee for one case was about 500 yen ($ 2.50).

A perfect bond of steel and concrete was assumed at the selected nodes and no bond was assumed in other places. In order to effect this particular bond behavior, the nodes of steel elements were connected to the nodes of concrete elements that were located at the same level as the center of steel elements.

5. EVALUATION OF THE ANALYTICAL RESULTS

5.1. Failure Mode and Ultimate Load

Failure modes predicted by the analysis, when the shear stiffness along the cracks is assumed to be zero, otherwize shear transfer across the cracks is ignored, are classified into three types : (a) diagonal compression failure of concrete above the support, (b) flexural compression failure of concrete at the section in the center of the span, and (c) flexural failure due to yielding of main reinforcing steel.

Four beams classified in diagonal compression failure have small shear span-depth ratios equal to 0.30 and 0.39 . Analytical results of these cases showed that the principal compressive stresses in the elements above the support were maximum among all elements. Stresses increased with applied enforced displacements and the elements gradually became plastic and softened. As a result, stress redistribution occurred. Stresses in adjacent elements increased and stress distribution became more uniform and the load carrying capacity of the beam became the maximum. When strains of softened elements above the support became very large

and stresses decreased extremely, stresses of other elements that had not yet been plastic began to decrease.

In the experiment, four beams, T2,T4,T5 and T6, which belonged to case (a) indeed failed in diagonal compression above the support. Observed failed portions of the specimen T5 is shown by shadow in Fig.6(a). Predicted results are very similar to observed results in failure mode and failed portions.

Analytical results of case (b) showed that the most critical stress state existed in the element of the top surface and at the span center where the moment is maximum. With an increase of applied displacement, stresses of the element increased and the element became plastic and softened. On the other hand, adjacent elements of top surface, which have the higher strength, nor the elements above the support did not become plastic.

In the experiments, three beams, T1,T3 and T7, which belonged to case (b), did not fail at the sections in the maximum moment region. Observed failed portions of the specimen T7 is shown by shadow in Fig.6(b). When cracks possessing an angle steeper than already existing diagonal cracks developed towards the edges of the bearing plate, slip occurred along this crack and the beam failed. This type of slip failure mode was not predicted by this analysis. This was considered to be due to the ignorance of the shear transfer. Therefore, trial calculations were executed on the assumption that the shear stiffness along the crack is made half of the uncracked one(α = 0.5 in equation 11). The results of calculations for T1 and T7 conformed that the secondary crack occurred in the point above the support at lower load than the ultimate load predicted by the analysis without shear transfer.

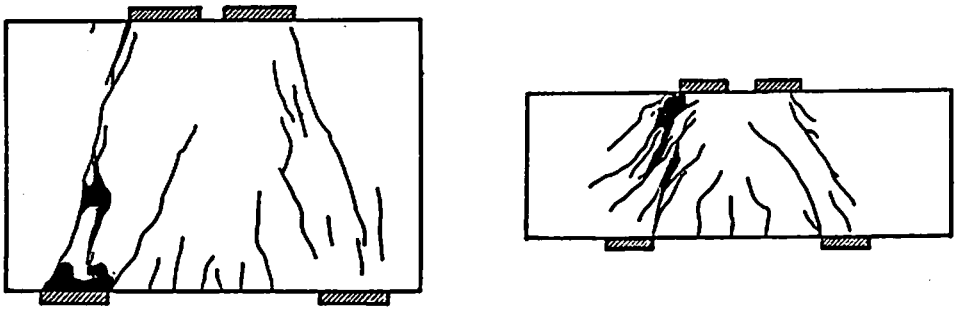

(a) T5, predicted to be failed in diagonal compression

(b) T7, predicted to be failed in flexural compression

Fig. 6 Crack Formation and Failed Portions

This will suggest that the proper modeling for shear transfer is extremely important for the analysis of this type of beams.

Results of analysis of case (c) showed that the beam failed in flexural mode governed by yielding of steel. The observed failure of T8, which belonged to case (c), was also in flexural mode.

Predicted failure modes and loads are given in Table 2 in comparison with the experimental values. The average ratio of the experimental ultimate load to the analytical one is 0.96 with the coefficient of variation of 0.18.

Table 2 Failure Mode and Ultimate Load

Beam	Failure Mode		Ultimate Load (KN)		
	expt.	anal.	expt.	anal.	expt./anal.
T1	SL	FC	629	506	1.24
T2	DC	DC	1028	1373	0.75
T3	SL	FC	228	235	0.97
T4	DC	DC	425	484	0.88
T5	DC	DC	1763	1930	0.91
T6	DC	DC	1155	996	1.16
T7	SL	FC	892	1221	0.73
T8	FT	FT	941	888	1.06

DC:Diagonal Compression
SL:Slip
FC:Flexural Compression
FT:Flexural Tension

5.2 Diagonal Cracking

According to the analysis two types of diagonal cracking mode was recognized. Four specimens, which had small a/d and belonged to case (a), and the rest, which had large a/d and belonged to case (b), showed different tendencies.

The analysis of small a/d specimens predicted that diagonal cracks developed dominantly while the development of flexural cracks was limited. On the other hand, in the analysis of large a/d specimens, diagonal cracks were distributed and developed uniformly in larger areas. Further, flexural cracks developed extensively. In Fig.7, predicted crack development of T5 as an example of small a/d specimens and T7 as an example of large a/d specimens are shown by broken lines. The load level in these figures is about 70% of analytical maximum load.

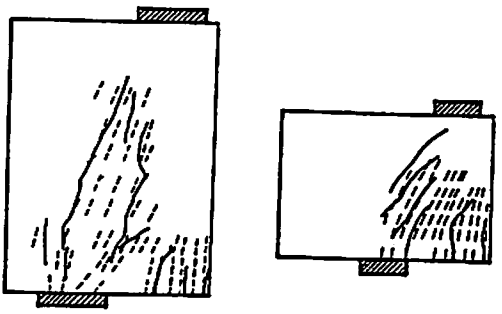

(a) T5 (b) T7

Fig. 7 Predicted and Observed Crack Pattern

In the experiments, development of dominant and long diagonal cracks were indeed characteristic of all small a/d beams and distributed diagonal cracks characterized large a/d beams. In Fig. 7,

development of observed cracks are superposed by bold lines. In both small and large a/d beams, positions of predicted and observed diagonal cracks are not necessarily coincident to each other. However, in consideration of the fact that crack evaluation points are discrete, the locations of cracks may be said to be similar. Moreover, directions of diagonal cracks are similar both in the prediction and in the observation. Therefore, it is deduced that this analysis can predict the actual behaviors reasonably accurately with regard to positions and directions of diagonal crack development for all the specimens.

5.3. Displacement and Strains of Concrete

The displacement of beam was satisfactorily predicted by the analysis. Fig.8 shows an example of the relationship between applied shear forces and the relative displacements of T5 specimen with the experimental values.

Fig.9 shows an example of the relationship between applied shear forces and the compressive principal strains of concrete just above the support. The tested values were obtained from the gauges attached to the surfaces of specimen T5. Fig.10 shows examples of strain distributions of Gauss points located at the same level of the concrete strut. These figures clearly show that strains of concrete and the displacement can be satisfactorily predicted by the analysis for the beams failed in diagonal compression mode.

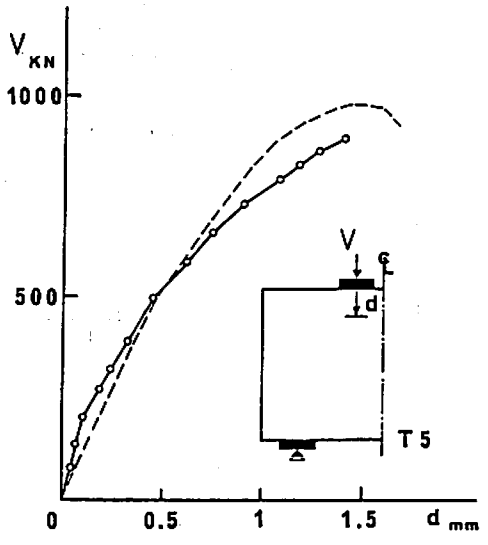

Fig.8 Shear-Displacement

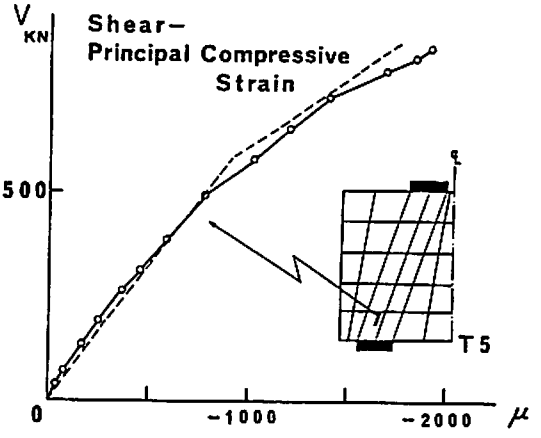

Fig.9 Shear-Compressive Strain

5.4. Evaluation of the Finite Element Analysis

Three types of failure mode were predicted by this analysis. In case (a), that is, diagonal compression failure mode of concrete above the support, the observed diagonal cracking pattern, stress distribution and failure mode were predicted reasonably accurately. Therefore, it is admitted that this analysis can estimate the actual behavior, on the whole, of this type of failure mode.

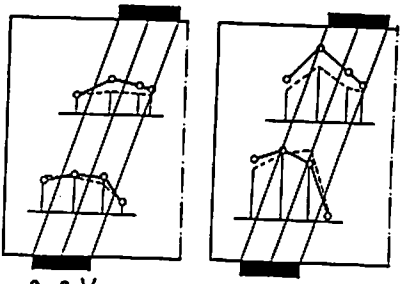

Fig.10 Strain Distribution in Concrete Strut

Secondly, in case (b), that is, flexural compression failure mode of concrete at the center span, the observed diagonal cracking pattern was predicted reasonably accurately but the variation of crack directions with load and failure mode could not be predicted by ignoring the shear stiffness along inclined cracks. Without shear transfer along the inclined crack surfaces, the stress condition in diagonal concrete struts bordered with diagonal cracks is almost uniaxial compression. When the shear stiffness is considered, there are additional shear stresses along the cracks and the resulting stress condition is severer (provided the existing compressive stress remains constant). Hence, the additional shear stress at crack surface results in undesirable stress condition in the diagonal concrete struts. The estimation of shear transfer along cracks is an important problem in order to predict the slip failure mode along a new surface inclined to the earlier cracks.

In case (c), that is, yielding of main reinforcement, the observed behaviors were adequately predicted.

6. CONCLUDING REMARKS

The behavior of reinforced concrete deep beams under increasing load was analyzed by a non-linear finite element method of analysis and the results were compared with experimental observations. For the loading tests of reinforced concrete deep beams the influencial parameters such as geometrical configuration, concrete strength and reinforcement ratio were varied so that various load carrying mechanisms can be observed. The bi-axial stress-strain relationship of concrete was expressed by a relation between stress and strain invariants developed herein. The following remarks appear to be relevant regarding the

techniques for non-linear method of analysis and capability of behavior prediction of deep beams.

(1). A step-iterative procedure of imposed displacement analysis was effective for solution of the behavior of structures where the portions were in strain softening region.

(2). The three failure modes observed on deep beam test specimens were, (a) crushing near the bottom of diagonal concrete struts, (b) slip along diagonal crack and (c) yielding of main reinforcement. The analysis was capable of predicting the two failure modes (a) and (c) described in (2). However, the failure mode (b), the slip along diagonal crack, was not predicted by the analysis. This may be due to the finite element idealization where the shear transfer resistance along the cracks was not assumed correctly, and thus resulting in different stress conditions in the diagonal struts which are vital load carrying member.

ACKNOWLEDGEMENTS

Dr. Jun Yamazaki, Associate Professor of Tokyo Metropolitan University, joined the discussions and gave valuable suggestions. Yutaka Ishikawa and Shin-ichi Inoue, undergraduate of our department, helped in executing the calculations. The program used in this analysis were developed from the program called FEMN (Finite Element Method of analysis for Non-linear problems) developed by the Non-linear Analysis Program Research Association. The authors express their gratitude for the warm and devoted cooperations.

REFERENCES

1. J.Eibl, "Application and Experimental Verification of Advanced Mechanics in Reinforced Concrete", Introductory Report IABSE Colloquium Delft 1981
2. H.Kupfer, H.K.Hilsdorf and H.Rusch, "Behavior of Concrete under Biaxial stresses", ACI Journal, Proceedings Vol. 66, No. 8, August 1969, pp.656-666
3. M.E.Tasuji, A.H.Nilson and F.O.Slate, "Biaxial Stress-Strain relationships for concrete", Magazine of Concrete Research, Vol. 31, No. 109, December 1979, pp217-224
4. H.Onuma and Y.Aoyagi, "Experimental Study on Ultimate Strength and Strain Behavior of Concrete under Biaxial Compressive Stresses, (in Japanese)", Report No.375016, Central Research Institute of Electric Power Industry, July 1976
5. M.D.Kotsovos and J.B.Newman, "A Mathematical description of the deformational behaviour of concrete under complex loading", Magazine of Concrete Research, Vol. 31, No. 107, June 1979, pp77-90